A spatially distributed hydroeconomic model to assess the effects of drought on land use, farm profits, and agricultural employment

M. P. Maneta,[1,2] M. O. Torres,[3,4] W. W. Wallender,[5,6] S. Vosti,[7,8] R. Howitt,[7] L. Rodrigues,[9] L. H. Bassoi,[10] and S. Panday[11]

Received 20 October 2008; revised 21 July 2009; accepted 5 August 2009; published 11 November 2009.

[1] In this paper a high-resolution linked hydroeconomic model is demonstrated for drought conditions in a Brazilian river basin. The economic model of agriculture includes 13 decision variables that can be optimized to maximize farmers' yearly net revenues. The economic model uses a multi-input multioutput nonlinear constant elasticity of substitution (CES) production function simulating agricultural production. The hydrologic component is a detailed physics-based three-dimensional hydrodynamic model that simulates changes in the hydrologic system derived from agricultural activity while in turn providing biophysical constraints to the economic system. The linked models capture the effects of the interactions between the hydrologic and the economic systems at high spatial and temporal resolutions, ensuring that the model converges to an optimal economic scenario that takes into account the spatial and temporal distribution of the water resources. The operation and usefulness of the models are demonstrated in a rural catchment area of about 10 km^2 within the São Francisco River Basin in Brazil. Two droughts of increasing intensity are simulated to investigate how farmers behave under rain shortfalls of different severity. The results show that farmers react to rainfall shortages to minimize their effects on farm profits, and that the impact on farmers depends, among other things, on their location in the watershed and on their access to groundwater.

Citation: Maneta, M. P., M. O. Torres, W. W. Wallender, S. Vosti, R. Howitt, L. Rodrigues, L. H. Bassoi, and S. Panday (2009), A spatially distributed hydroeconomic model to assess the effects of drought on land use, farm profits, and agricultural employment, *Water Resour. Res.*, *45*, W11412, doi:10.1029/2008WR007534.

1. Introduction

[2] Demands on freshwater resources are increasing worldwide, and in many areas, water supply is a major limiting factor for agricultural development [*The World Bank*, 2007] with possible negative direct and indirect implications for rural poverty. An interdisciplinary assessment of how farmers may react to different water policies or environmental scenarios (such as a period of drought) is important from a management point of view, as it may lead to more effective and better targeted actions.

[3] Interdisciplinary models involving hydrology, ecology, economy, and/or sociopolitical aspects have been developed to solve a variety of water-related problems. Examples are those intended to investigate optimal strategies for water allocation and use between multiple competing sectors [*Cai*, 2008; *Cai et al.*, 2003b; *Rosegrant et al.*, 2000; *Ward and Lynch*, 1996], for conjunctive surface water–groundwater use [*Burt*, 1964; *Harou and Lund*, 2008; *Pulido-Velazquez et al.*, 2004, 2006], for water pricing, irrigation productivity, and institutional constraints [*Characklis et al.*, 1999, 2006; *Lefkoff and Gorelick*, 1990a, 1990b; *Vaux and Howitt*, 1984], or to investigate ecological and economical aspects [*Loucks*, 2006; *Voinov et al.*, 1999]. An extensive survey of hydroeconomic models applied to different problems is given by *Harou et al.* [2009].

[4] *Noel and Howitt* [1982] and *Lefkoff and Gorelick* [1990b] present early examples of linked hydroeconomic models with an agronomical functions to study water transfers and allocation as well as water quality. More recently, aiming at large-scale systems, *Rosegrant et al.* [2000] and *Cai et al.* [2003a] highlighted the role of water and salt transport to evaluate soil salinity and water availability usable for irrigation, and *Guan and Hubacek* [2007] investigated the feedback between economic activity and water quality. Others such as *Krol et al.* [2006], *Medellín-Azuara et al.* [2008], or *Harou et al.* [2006] focused on the impacts of drought and climate change on water availability, agriculture,

[1]Geosciences Department, University of Montana, Missoula, Montana, USA.
[2]Formerly at Department of Land, Air and Water Resources, University of California, Davis, Davis, California, USA.
[3]Department of Economics, Catholic University of Brasília, Brazilia, Brazil.
[4]Formerly at Department of Agricultural and Resource Economics, University of California, Davis, California, USA.
[5]Department of Land, Air and Water Resources, University of California, Davis, California, USA.
[6]Also at Department of Biological and Agricultural Engineering, University of California, Davis, California, USA.
[7]Department of Agricultural and Resource Economics, University of California, Davis, California, USA.
[8]Also at Center for Natural Resources Policy Analysis, University of California, Davis, California, USA.
[9]Embrapa Cerrados, Planaltina, Brazil.
[10]Embrapa Semiárido, Petrolina, Brazil.
[11]AMEC Geomatrix Consultants, Inc., Herndon, Virginia, USA.

0043-1397/09/2008WR007534$09.00

Table 1. Decision Variables Included in the Economic Model of Agriculture

Decision Variable	Supply Limit
Nonirrigation Inputs	
Land	constrained
Fertilizers	unconstrained
Pesticides	unconstrained
Seeds	unconstrained
Nonirrigation hired labor	unconstrained
Nonirrigation family labor	constrained
Machinery	unconstrained
Irrigation Inputs	
Surface water	constrained
Groundwater	constrained
Irrigation hired labor	unconstrained
Irrigation family labor	constrained
Capital	unconstrained
Electricity/energy	unconstrained

and other socioeconomic characteristics. The models varied in approach and level of complexity according to the problem to be analyzed. In general, approaches using complex distributed hydrologic models need an externally linked solution (only model outputs are exchanged) between the hydrologic and the economic components [e.g., *Lefkoff and Gorelick*, 1990b; *Noel and Howitt*, 1982], whereas coupled systems integrated in a single set of equations are only possible by greatly simplifying the hydrologic component [e.g., *Cai et al.*, 2003a; *Guan and Hubacek*, 2007]. In this approach the components may transfer and share implicitly both outputs and internal variables, allowing for simultaneous and more robust implicit solutions of the optimization problem. However, this is done at the expense of potentially drastic spatial and temporal aggregation of the hydrologic model, missing the chance to study the problems at the scale in which hydrology becomes relevant for small farms.

[5] At the community scale, different farms may compete for the available water resources. The spatial location of the farms with respect to the water sources matters, especially in configurations in which demand is satisfied in a cascading manner along a river. Similarly, groundwater drawdown due to pumping by large-scale farmers may have spatial impacts that may negatively affect smaller neighboring farmers. Also, the availability of the water resources changes over time, and this seasonality affects the cropping strategy of farmers. These effects can be studied only by using a detailed distributed and physics-based description of the hydrologic system at the appropriate spatial and time scales.

[6] If the hydrologic module cannot provide information at a resolution that properly captures the variability of the constraints in space and in time, the optimization of the economic inputs may converge to a scenario that is not hydrologically feasible even though it is within the constraints imposed by the hydrologic model. This is because the hydrologic modules of previous formulations do not take into account the spatial and temporal distribution of water within the landscape at the required resolution. For instance, while a region may overall have enough water to cover the seasonal demand, this water may be unevenly distributed in the landscape or unevenly distributed in time so that some farms may not have access to it when they need it.

[7] In this paper we present a hydroeconomic model that links a three-dimensional (3-D) comprehensive physics-based hydrologic model [*Panday and Huyakorn*, 2004] with a nonlinear agricultural economics model based on positive mathematical programming [*Howitt*, 1995] that simulates farmer economic behavior and agricultural production processes. The linkage between the two models is an example of how the gap between models that operate at disparate temporal and spatial resolutions can be bridged using an approach different from the penalty approach used by *Cai* [2008]. The physical base and high spatial and temporal resolution of the hydrologic model allow for a rigorous evaluation of how the spatiotemporal heterogeneity of the environmental factors affects water availability at any point in the landscape and how this affect farmers' economic behavior.

[8] Although multi-input and crop-specific production functions have been used in the context of hydroeconomic modeling before [e.g., *Cai and Wang*, 2006; *Cai et al.*, 2008; *Marques et al.*, 2006; *Ringler et al.*, 2006], the production function implemented in the presented model explicitly incorporates effective precipitation as an argument into the production function, improving the approach of *Brown and Rogers* [2006] and *Brown et al.* [2006]. In addition it relaxes the assumption of fixed technical coefficients used by *Guan and Hubacek* [2007] and allows farmers to control input substitution and to change crop mix and input mix.

2. Economic Model of Agriculture

[9] The economic model proposed here is based on a class of models commonly referred to as positive mathematical programming, or PMP [*Howitt*, 1995], and widely used in applied research and policy analysis [*House*, 1987; *Howitt and Gardner*, 1986; *Kasnakoglu and Bauer*, 1988; *Lance and Miller*, 1998].

2.1. The Objective Function

[10] In order to set up the analytical model, it is assumed that farmers seek to maximize net benefits derived from their farming activities in a given year. That is,

$$\max\ net = \sum_i \left[p_i q_i(X_{ih}, P_i) - \sum_h \left(p_h X_{ih} - \alpha_i X_{iland} - 0.5\psi_i X_{iland}^2 \right) \right] \quad (1)$$

The first term in equation (1) represents the farmer's revenue derived from agricultural activity, where p_i is the output price of crop product i, which is produced according to a production function $q_i(X_{ih}, P_i)$ to be described in more detail in section 2.2; X_{ih} is an $i \times h$ matrix that contains information on the h agricultural inputs corresponding to each crop i. The agricultural inputs are the decision variables that the farmer can control to maximize revenues and include land, pesticides, fertilizers, seeds, hired labor for irrigation and nonirrigation, family labor for irrigation and nonirrigation, machinery, electricity used in irrigation, surface water, groundwater, and irrigation capital (Table 1); P_i is the amount of effective precipitation (precipitation reaching the soil storage used by plants) over the area covered by crop i during its growing season. Note that P_i has a seasonal temporal resolution and therefore captures the rainfall conditions of the period of the year in which the crop is planted.

[11] The cost to produce crop i is defined by the last three terms of equation (1). The second term is the market prices of inputs p_h multiplied by the quantity of inputs used to grow crop i. The third term is the implicit cost associated with land allocation. It has a quadratic specification with parameters α_i and ψ_i and incorporates the increasing marginal costs associated with allocating increasing amounts of land to a particular crop [*Howitt*, 1995]. An example of an implicit land allocation cost is land quality heterogeneity. As a given farmer allocates increasing amounts of land to a specific crop, the new land may be of inferior quality and hence crop yield may fall.

[12] While the price of most agricultural inputs (p_h) is fixed, the cost of groundwater depends on its accessibility. Farmers using groundwater pay a unitary price p_{gw} derived from the total cost of groundwater pumping (c_{gw}) and the depth to water table, which is defined as follows:

$$c_{gw} = \beta \cdot \left(\sum_i gw_i \cdot depth \right), \quad (2)$$

where β reflects the electrical energy required to pump one unit of groundwater and other unitary costs associated with extracting water from a well, $\sum_i gw_i$ is the amount of groundwater pumped for all crops i, and depth is the depth to the water table. In this context, p_{gw} is equal to the derivative of equation (2) with respect to the amount of groundwater pumped; that is,

$$p_{gw} = \beta \cdot depth. \quad (3)$$

[13] In modeling perennial tree crop production, we follow the method used by *Chatterjee et al.* [1998], in which perennial crop output is based on "average" production over trees of different ages. Also, no lags between observed price changes and their realized impacts are explicitly included, and the decision-making process modeled is neither designed under uncertainty nor based on expectation formation. Impacts of changes in relative output and input prices, on land allocation to perennials, and on their yields and input use are based on the assumption that farmers can change the land allocation to perennial crops as quickly as to any annual crop, and that they look at observed rather than expected output/input prices.

2.2. Production Function

[14] The production function $q_i(X_{ih}, P_i^a)$ is used to estimate the agricultural production of crop i given the set of agricultural inputs X_{ih} and amount of actual precipitation P_i^a over crop i. A quadratic form of production function together with a maximum entropy estimation method is commonly found in previous hydroeconomic models [*Cai and Wang*, 2006; *Cai et al.*, 2008; *Howitt and Msangui*, 2002; *Marques et al.*, 2006; *Ringler et al.*, 2006]. While the flexibility of the quadratic specification is theoretically desirable, it has practical drawbacks in that, to date, no one has shown how to bound the estimates of the elasticity of substitution when using maximum entropy estimates of a production function. Accordingly, we decided to use the more restrictive constant elasticity of substitution (CES) specification that enables us to impose prior values for the elasticity of substitution on the calibration of the production function. Given the micro data sets that are used in this study, we are confident that the prior specification of elasticities of substitution is preferable to unbounded estimates.

[15] The form of the CES used, though, is adapted according to whether the crop is rain-fed or irrigated. If the crop is rain-fed, the production function is

$$q_i^r = A_i Precip_i \left(\sum_h b_{ih-6} X_{ih-6}^{\gamma} \right)^{\frac{\varepsilon_i}{\gamma}}, \quad (4)$$

where the superscript r stands for rain-fed production function; A_i, and the share parameters b_{ih}, are production function parameters; $\gamma = (\sigma - 1)/\sigma$; σ is the elasticity of substitution among inputs; and ε_i is the return to scale parameter. The subscript $h - 6$ indicates that rain-fed crops do not use the six irrigation inputs used exclusively in the irrigation systems such as hired labor and family labor for irrigation, electricity used in irrigation, surface water, groundwater, and irrigation capital. $Precip_i$ is defined as the ratio between the actual over the expected (e.g., average) amount of precipitation, that is, $Precip_i = P_i^a / P_i^e$.

[16] If the crop is irrigated, the function is

$$q_i^{ir} = A_i \left(\sum_h b_{ih-2} X_{ih-2}^{\gamma} + b_w \left(X_{isw} + X_{igw} + P_i^a \right)^{\gamma} \right)^{\frac{\varepsilon_i}{\gamma}}, \quad (5)$$

where the superscript ir stands for irrigation production function; A_i, and the share parameters b_{ih-2}, are production function parameters. The subscript $h - 2$ indicates that the parameters are for all agricultural inputs h except surface and groundwater; b_w is the share parameter associated with applied water used in the irrigation whether it comes from surface water X_{isw}, groundwater X_{igw}, or actual precipitation. In total there are 12 share parameters in the irrigation production function.

2.3. Shadow Prices for Constrained Inputs

[17] In the case of inputs with limited supplies such as family labor, surface water and groundwater, or land, the marginal cost of an input is represented by the sum of its market price plus its shadow price, λ. The shadow prices for each nontraded or limited input are the Lagrange multipliers that solve a linear programming model, which has as its explicit objective the maximization of net income using land allocation as the decision variable

$$\max_{land} \sum_i p_i \hat{y}_i X_{i\,land} - \sum_i \left(p_h a_{ih} X_{i\,land} \right) \quad (6)$$

subject to farm-level resource constraints

$$\begin{cases} \text{Land} : \sum_i X_{i\,land} \le B_{land}, \\ \text{Family labor} : \sum_i a_{ifl} X_{i\,land} \le B_{fl}, \end{cases} \quad (7)$$

$$\begin{cases} \text{Surface Water} : \sum_i X_{i_{sw_m}} \le B_{sw_m}, \\ \text{Groundwater} : \sum_i X_{i_{gw_m}} \le B_{gw_m}, \end{cases} \quad (8)$$

and a model calibration constraint

$$X_{i\,land} \le \hat{X}_{i\,land}, \qquad (9)$$

the new symbols being $\hat{y}$, the yield per hectare of land dedicated to crop i, and a_{ifl}, the amount of family labor used per hectare (X_{ifl}/X_{iland}). B_{land}, B_{fl}, B_{swm}, and B_{swm} are the total availability of land, family labor, surface water, and groundwater, respectively. The subscript m in equation (8) indicates that the constraints are given for each month m. Equations (8) and (9) assure that the total amount of land, family labor, surface water, and groundwater used do not exceed the available amounts. In equation (9), $\hat{X}_{iland}$ is the total amount of land allocated to crop i that is observed by researchers; this constraint prevents specialization and preserves observed crop allocation patterns while estimating shadow values of limited or nonmarketed inputs.

[18] In the resulting Lagrangian function, the Lagrange multipliers are the shadow values (λ_{land}, λ_{fl}, λ_{sw}, and λ_{gw}) associated with the resources constraints (equations (7) and (8)) and are needed in the calibration of the production function (Appendix A). For the model calibration constraint (equation (9)), the associated Lagrange multiplier, say, $\lambda_{i_{land}}$, measures how much farmers gain by reallocating one unit of land from the least profitable crop to a more profitable crop i (see section 3). Notice that although the shadow values associated with the fixed supply resources such as land, family labor, and water may change from farmer to farmer and are not crop specific, the Lagrange multiplier associated with equation (9) is farmer and crop specific.

[19] To operate within the constraints set out in equation (8) at a monthly time step, information is collected on the dates of planting and harvesting for each crop i, and for each farmer during the 365 days (n) of the year. Then, assuming that each crop has four growth stages, each with an associated water crop coefficient kc and using the reference crop evapotranspiration Eto method [*Allen et al.*, 1998], the agronomicaly optimal evapotranspiration for each crop i on day n is $kc_{in}Eto_n$. For those days in which $kc_{in}Eto_n > P_n^a$, call Z_{in} the difference between $kc_{in}Eto_n$ and P_n^a, $Z_{in} = kc_{in}Eto_n - P_n^a$. For $kc_{in}Eto_n < P_n^a$, Z_{in} is truncated at 0. The sum of Z_{in} annually takes then the form of $\sum_{n+1}^{365} Z_{in}$, where $n = 1$ refers to 1 September, and monthly, the form of $\sum_{n=s}^{f} Z_{in}$, where s and f are the starting and ending day, respectively, of each month.

[20] Using these annual and monthly sums of Z_{in}, we can calculate the percentage of water demand per crop i per month m (Met_{im}) as the monthly share of the total water deficit:

$$Met_{im} = \frac{\sum_{n=s}^{f} Z_{i_n}}{\sum_{n=1}^{365} Z_{i_n}}, \qquad (10)$$

where $m = 1, \ldots, 12$ (month 1 refers to 2 September to 3 October to November and so on). The optimal amount of applied surface water and groundwater allocated to crop i in month m is $X_{i_{sw_m}} = Met_{i_m} X_{i_{sw}}$ and $X_{i_{gw_m}} = Met_{i_m} X_{i_{gw}}$.

[21] The total amount of water used in month m to produce crop i, which can come from surface water and from groundwater sources, is

$$\sum_i X_{isw_m} + \sum_i X_{igw_m} = \sum_i Met_{i_m} * \left(a_{i_{sw}} + a_{igw} \right) * X_{iland}, \qquad (11)$$

where a_{isw} and a_{igw} are respectively the seasonal amounts of surface water and groundwater applied per hectare (X_{isw}/X_{iland}) and (X_{igw}/X_{iland}), respectively. Equation (11) together with equations (7), (8), and (9) form the set of constraints for the linear optimization problem.

3. Implementation of the Economic Model of Agriculture and Estimation of Parameters

[22] The parameters for the CES production function (equations (4) and (5)) are found experimentally. Estimation of the full set of parameters for the production function with seven inputs in equation (4) requires each crop i to be parameterized in terms of seven share parameters b_{ih-6}, one return to scale parameter ε_i, and the crop-specific parameter A_i; and 12 share parameters b_{ih}, one returns-to-scale parameter ε_i, and the crop-specific parameter A_i in equation (5). For the estimation of the parameters, $Precip_i$ is set to a value of 1.

[23] Typically, the very limited degrees of freedom available for parameter estimation may require their estimation by methods such as maximum entropy [*Golan et al.*, 1996; *Jaynes*, 1957; *Mittelhammer et al.*, 2000; *Paris and Howitt*, 1998]. In this paper we follow an analytical rather than an econometric approach in which the parameters are calculated using economic optimality conditions. We assume that there is no difference between the marginal productive effects between groundwater, surface water, and precipitation (i.e., $\partial q_i/\partial sw_i = \partial q_i/\partial gw_i = \partial q_i/\partial P$).

[24] Formally, the optimality equations for each input can then be defined as

Unconstrained inputs

$$p_i \frac{\partial q_i}{\partial X_{iu}} = p_u$$

Irrigation and nonirrigation family labor

$$p_i \frac{\partial q_i}{\partial X_{i\,fl}} = \lambda_{fl}$$

Land

$$p_i \frac{\partial q_i}{\partial X_{i_{land}}} = p_{land} + \lambda_{land} + \lambda_{i_{land}}$$

Surface water

$$p_i \frac{\partial q_i}{\partial X_{i_{sw}}} = p_{sw} + \lambda_{sw}$$

Groundwater

$$p_i \frac{\partial q_i}{\partial X_{i_{gw}}} = \beta \cdot depth + \lambda_{gw}. \qquad (12)$$

[25] For the unconstrained inputs (identified by subscript u), the unitary costs are simply their market price. For the constrained inputs each unitary cost is the sum of their purchase price and shadow values λ_{land}, λ_{fl}, λ_{sw}, and λ_{gw}, respectively. In addition, in the case of land there is a further marginal cost component $\lambda_{i_{land}}$ that is crop and farmer specific. This component results from the calibration constraint represented by equation (9). Thus the total marginal cost associated with land allocation to crop i is composed of the amount a farmer pays per hectare (market price), plus the shadow value λ_{land} representing resource constraints, plus another shadow value $\lambda_{i_{land}}$ representing the increasing marginal cost of assigning new land to crop i.

[26] Subscript u in the previous equation indicates the unconstrained inputs in X (i.e., fertilizers, pesticides, seeds, hired labor, hired labor for irrigation management, machinery, capital, and electricity). By algebraically manipulating the optimality equations, we reach expressions for each of the parameters $\hat{b}_{ih}$, and A_i as functions of input prices, output prices, and input quantities (see Appendix A). For this exercise we assume constant returns to scale for all crops ($\varepsilon_i = \varepsilon = 1$) and a value of 0.25 for the elasticity of substitution (σ). In the current model we further assume one elasticity of substitution for all inputs (they can be all equally substituted). For the calculation of parameters α_i and ψ_i of equation (1), see Appendix B.

4. Economic Model at Simulation Time

[27] Equation (13) uses the parameterized CES production function $\hat{q}$ (for irrigated and nonirrigated crops) to find the optimal set of inputs that maximizes net revenues

$$\max_{\mathbf{X}} \sum_i \left(\left[p_i \hat{q}_i^r(X_{ih}, P_i) + p_i \hat{q}_i^{ir}(X_{ih}, P_i) \right] - \sum_h \left(p_h X_{ih} - \hat{\alpha}_i X_{i_{land}} - 0.5 \hat{\psi}_i X_{iland}^2 \right) \right) \quad (13)$$

when farmers are subject to resource and water availability constraints:

$$\text{Land} \qquad \sum_i X_{i_{land}} \le B_{land}$$

$$\text{Family labor} \qquad \sum_i X_{i_{fl}} \le B_{fl}$$

$$\text{Surface water} \qquad \sum_i X_{isw_m} \le B_{sw_m}$$

$$\text{Groundwater} \qquad \sum_i X_{igw_m} \le B_{gw_m}$$

$$\sum_i X_{isw_m} + \sum_i X_{igw_m} = \sum_i Met_{i_m} \quad X_{i_{sw}} + X_{i_{gw}} \quad (14)$$

Unlike in equations (7) and equation (11), equation (14) does not use fixed amounts per hectare but total inputs, indicating that the assumption of fixed input proportions has been relaxed. The subscript m indicates that the water constrains are given on a monthly basis for each water source.

5. Hydrologic Model

[28] In order to simulate the spatial and temporal impact of water reallocation derived from agricultural activities, a fully coupled physics-based 3-D hydrologic model [*HydroGeoLogic, Inc.*, 1996; *Panday and Huyakorn*, 2004] was used. The hydrologic model uses finite differences to solve a two-dimensional form of the diffusion wave approximation of the Saint-Venant equation for surface flows, a 1-D solution of the diffusion wave for channel flow, and a 3-D solution for variably saturated soils of Richards' equation to simulate subsurface flows. By solving Richards' equation for variably saturated flows, the entire subsurface domain (saturated and nonsaturated) is solved simultaneously with the same equation. The interaction terms between the three domains that allow their coupling are [*HydroGeoLogic, Inc.*, 1996]

$$\begin{aligned} q_{gc} &= K_c\ (h_c - h_g) = Q_{gc}/L\mathrm{P}_{ups} \\ q_{go} &= K_g\ (h_o - h_g) = Q_{go}/(\Delta x \Delta y) \\ q_{oc}^{free} &= C_d \sqrt{2g} (h_o - Z_{bank})^{3/2} = Q_{oc}^{free}/(\Delta x \Delta y), \end{aligned} \quad (15)$$

where q_{gc} indicates fluxes between groundwater and channel [LT^{-1}], K_c is a conductance coefficient [T^{-1}], h_c is hydraulic head in the channel [L], h_g is hydraulic head in the subsurface system [L], Q_{gc} is the volumetric flow across the boundary [$\mathrm{L}^3\ \mathrm{T}^{-1}$], L is the length of the reach segment [L], and $\tilde{\mathrm{N}}_{ups}$ is the upstream wetted perimeter [L]; q_{go} is the flux between the subsurface and the surface domain [LT^{-1}], K_g is a conductance coefficient across the boundaries [T^{-1}], h_o is the head at the surface [L], Q_{go} is the volumetric flux across the boundary [$\mathrm{L}^3\ \mathrm{T}^{-1}$], and $\Delta x \Delta y$ is the area of the cell through which the interaction occurs [L^2]. The interaction between the overland flow and the channel flow domains are given by q_{oc}^{free} in case the interaction can be described as a free-flowing weir (channel discharge is below the banks, no flooding) [LT^{-1}]; C_d is the weir discharge coefficient [], g is the gravitational constant [LT^{-2}], Z_{bank} is the channel bank elevation [L], and Q_{oc} is the volumetric flow across the bank [$\mathrm{L}^3\ \mathrm{T}^{-1}$].

[29] The flow through the well is governed by a 1-D variably saturated flow equation [*HydroGeoLogic, Inc.*, 1996]:

$$\frac{\partial}{\partial l}\left(\frac{\rho g}{8\mu} r_w^2 k_{rw} \frac{\partial h_w}{\partial l}\right) = \frac{\partial S_w}{\partial t} + S_w S_s \frac{\partial h_w}{\partial t}, \quad (16)$$

where l is distance along the well screen [L], ρ is the density of water [ML^{-3}], μ is the viscosity of water [$\mathrm{ML}^{-1}\ \mathrm{T}^{-1}$], r_w is the radius of the well [L], k_{rw} is the relative permeability within the well cell, S_w is the dimensionless saturated thickness of the well cell (ratio of saturated thickness to cell thickness), S_s is the wellbore specific storage [L^{-1}], and h_w is the hydraulic head in the well [L]. Water withdrawals are applied to the bottommost screened node of the well and the formulation appropriately distributes the contribution of each

screened node to the well yield. A variety of modules are included to simulate wells, weirs, reservoirs, water diversions, and other hydraulic structures [*HydroGeoLogic, Inc.*, 1996].

[30] The hydrologic model operates in stress periods similar to MODFLOW [*McDonald and Harbaugh*, 1988]. A stress period is defined as a time span in which the boundary conditions of the system are constant throughout the spatial domain. Conveniently and unlike MODFLOW, transient boundary conditions (precipitation and reference evapotranspiration) can be entered in the hydrologic model using time series with arbitrary time resolution within stress periods.

6. Model Linkage

6.1. Common Terms

[31] During a simulation run, the economic model solves for the values in the input matrix X_{ih} that maximizes equation (13). The optimized applied water for each crop using its optimal proportions of surface water X_{isw} and groundwater X_{igw} as well as the optimized land allocated for each crop X_{iland} provides the common terms connecting the economic model to the hydrologic model.

[32] This information is used to calculate the rates of applied water for each crop, the water diversions from the reservoirs or wells, and the area dedicated to each crop, which are the needed boundary conditions to run the hydrologic model and that provide the link from the economic to the hydrologic module. The rate of applied water (R) per unit area on crop i at growth stage u is calculated as proportional to the crop coefficient at u:

$$R_{i_u} = \frac{X_{i_{aw}}\left(kc_{i_u} \Big/ \sum_u kc_{i_u}\right)}{X_{i_{land}} \cdot \Delta t_{i_u}}, \qquad (17)$$

where kc_{iu} is the given crop coefficient for crop i during growing stage u, X_{iaw} is total applied water to crop i ($X_{iaw} = X_{isw} + X_{igw}$), and Δt_{iu} is the time length of the growth period u for crop i. Therefore water is assumed to be evenly applied within each growing stage but can be different across growth stages.

[33] The water diversion rate D from each water source w (surface reservoirs or wells) at a given stress period t is calculated as the sum of the water demand from that source:

$$D_{wt} = \begin{cases} \left(\sum_{i \text{ retrieving water from } w} \left(R_{i_u} X_{i_{land}} \left(sw_i \Big/ (X_{i_{aw}} n_{i_{sw}})\right)\right)\right)_t & \text{if surface water} \\ \left(\sum_{i \text{ retrieving water from } w} \left(R_{i_u} X_{i_{land}} \left(gw_i \Big/ X_{i_{aw}} n_{i_{gw}}\right)\right)\right)_t & \text{if groundwater} \end{cases}, \qquad (18)$$

where $n_{i_{sw}}$ is the number of surface water sources and $n_{i_{gw}}$ is the number of groundwater sources involved in the water supply to crop i at a given period t and ($sw_i/X_{iaw}n_{igw}$) and ($gw_i/X_{iaw}n_{igw}$) are the proportion of total demand that would correspond to each surface and groundwater source, respectively. A computer program was developed to read the output of the economic model and produce the necessary 2-D arrays (raster layers) needed to run the hydrologic model. The land allocated to each crop is given by the economic model as a proportion of the total arable land in each farm. Going from top to bottom and left to right in the raster image, pixels in the farm that are not already assigned to a crop are allocated to the new crop until the optimal allocated area is achieved. Similarly, a set of layers holding the values of R at each growth period u are given for each pixel associated with crop i are created and information on the values of D for each water source w at each period t is also properly formatted to be used by the hydrologic module. This computer program facilitates the iteration processes by taking the required information from the economic model and outputting the set of raster layers with spatial information in a format ready to be used by the hydrologic model.

[34] Once the hydrologic model is run, the water constraints calculated by the hydrologic model provide the link between the hydrologic and the economic model closing the iteration loop. The constraints for each surface water source (potential water availability) to the economic model are approximated by aggregating per month the incoming flux information

$$B_{sw_m} = S_{o_{m_1}} + \int_{t=m_1}^{m_2} Q_{in}(t)dt, \qquad (19)$$

where B_{sw_m} is the total potential surface water available for a given source (lake, pond, river reach) at month m, $S_{o_{m_1}}$ is the water stored in the source at the beginning of month m_1, m_2 indicates the time at the end of the month, and Q_{in} is the incoming discharge to the source.

[35] Similarly, the maximum potential available groundwater during month m is approximated by multiplying the wetted perimeter of the well times the average hydraulic conductivity of the soil around the well (K_s), δ_m being the distance between the water surface in the well and the well bottom and r_ω being the radius of the well:

$$B_{gw_m} = \delta_m \cdot 2\pi r_\varpi \cdot K_s \cdot (m_2 - m_1). \qquad (20)$$

Note that only an approximation is needed since the actual water availability will be calculated and updated each time the hydrologic model is run. Convergence is discussed later.

6.2. Bridging Between Disparate Time and Spatial Model Resolutions

[36] One requirement for model linkage is to bridge the different spatial and temporal resolutions at which each model operates. The economic model operates at a spatial resolution corresponding to the farm or household level while its temporal resolution is a year, although it operates implicitly using monthly information on water availability. The hydrologic model typically operates at a finer spatial and temporal resolution. Depending on the size of the basin, the volumetric grid size used to partition the space ranges from decameters to 1 km on the sides and from decimeters to several meters in depth. The temporal resolution is determined by the speed at which the processes occur, typically minutes to hours.

[37] The economic model is technically nonspatial. The relative position of the farms is implicit in the water con-

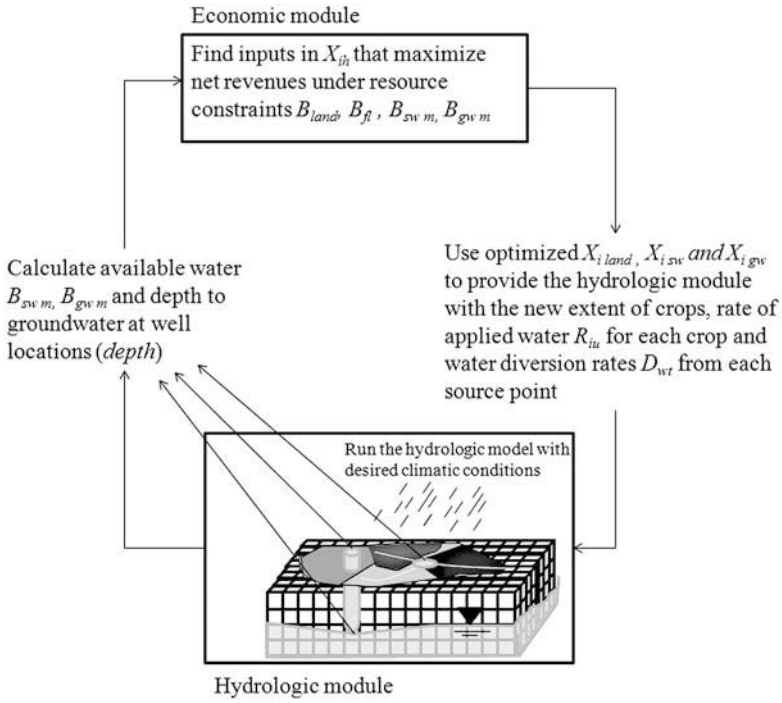

Figure 1. Schematic of the loop between the hydrologic and the economic model of agriculture. The modules iterate until the economic model converges to a state that is consistent with the available resources.

straints (farmers at the end of the pipeline or water sources with smaller contributing areas will face tighter water constraints). In addition, it captures implicit temporal information about planting dates for crops through their different calculated water demands (crops in the dry months will need more supplemental water). Spatial and temporal coherence of the system is therefore kept by the spatially distributed hydrologic model because it explicitly contains spatial and temporal information about the landscape and the boundary conditions. Setting the initial crop mix and planting calendar similar to the observed and agricultural activities ensures that the models captures what the farmers actually did during the survey period. In the economic model the watershed is disaggregated according to categories of farmers, determined by the size of the farm.

[38] Figure 1 summarizes the linking scheme. When the hydrologic model is run, the available water for irrigation from surface water and from groundwater via depth to the water table (in the case of wells) are calculated at the point sources (wells, lakes, etc.) and the time series are aggregated to provide the economic models with monthly information on available water volume and average water table depths. The economic model then operates with that information and recalculates the optimal cropping mix and use of water. Once the new crop scenario is calculated, the spatial and temporal information, contained in an aggregated form in the economic model, is restored in the hydrologic model. The generated information provides the hydrologic model with updated crop areas, updated water diversions from the different sources, and updated applied water per crop. This process is run iteratively until convergence occurs. The system converges when for nonwater-binding conditions the changes in cropped areas are smaller than a predefined percentage or, in the case of binding (water restricted) conditions, when the water demand for the optimal crop mix is met by the hydrologic system.

6.3. Iteration Procedure During Model Run

[39] The model interaction occurs explicitly in a linked scheme, so the models are run sequentially and the feedback information is updated after each model run. The economic model provides the boundary conditions to the hydrologic model, which in turn provides the water constraints to the economic model as previously explained.

[40] During the first iteration, the hydrologic model is run with no water diversions and no applied irrigation water (a hydrologic system without agricultural load). The simulated flows and water table depth in wells represent the water availability under natural conditions, which is aggregated by month using equation (19) and equation (20). This information is used in the economic model (as restrictions in water availability implemented in equation (14)) to produce the optimal crop pattern with the available water according to the production functions (q_i). The crop areas, applied water, and the surface water–groundwater trade-off calculated by the economic model are used to calculate the rate of applied water and rate of water diversions from the different water sources in the hydrologic model using equation (17) and equation (18). The hydrologic model is run to test the feasibility of the scenario and evaluate the hydrologic impact of the water allocation. Farmers diverting from sources upstream are optimized first.

[41] Because total inflows are not evenly distributed during a month and flows fluctuate about the average, instantaneous potential water availability may be different from monthly average potential water availability. Thus, unless a large reservoir functions to provide steady water availability,

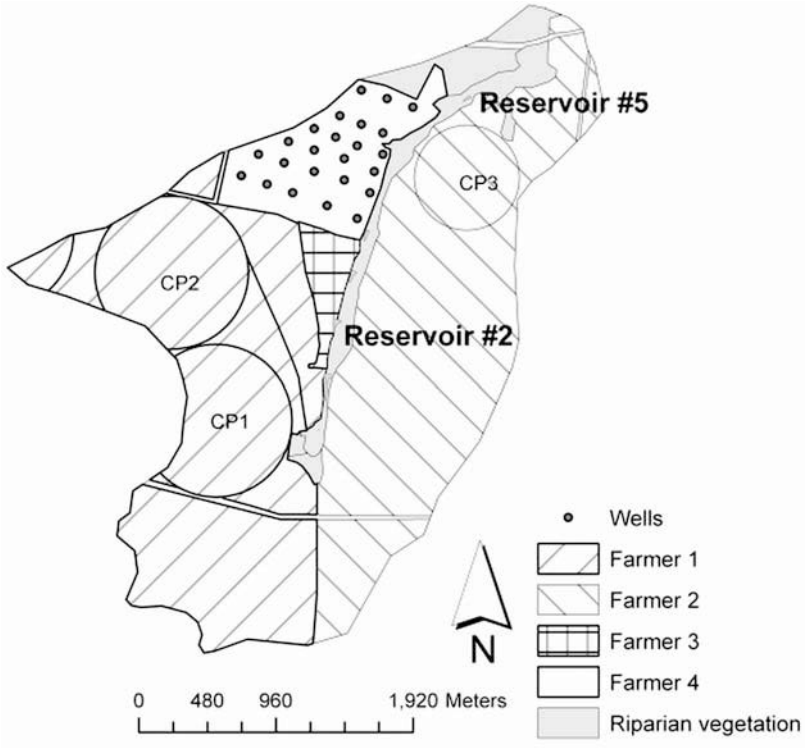

Figure 2. Location of farmers, center pivots, reservoirs, and wells within the Buriti Vermelho catchment area.

the water that can be diverted at a specific rate may be determined by the lower flows and therefore be smaller than the potential water availability as calculated by equation (19). In that case, especially when water availability is binding, a farmer may not be able to sustain the irrigation at the optimal rate predicted by the economic model because this prediction is based on steady monthly potential water availability rather than on instantaneous potential water availability. Because this problem is difficult to solve given the disparate temporal resolutions of the economic and hydrologic models, a heuristic approach is used in order to calculate optimal water application according to actual availability. When the calculated water diversion rate cannot be sustained during a month, the original potential water availability used by the economic model for this month is decreased by a small arbitrary value (e.g., 10%) and the crop areas, amount of applied water and its surface–groundwater trade-off are recalculated using the economic model.

7. Modeling Scenario

[42] In order to test the model, a demonstration setup using information obtained for a rural watershed in Brazil was used. This rural catchment (Figure 2), located near Brasília, is a first-order basin of 9,407,100 m^2. Its climate is tropical, with a clearly defined dry season during the Brazilian winter months of June through September. Supplemental irrigation during this season offers the potential to expand the production and increase net profits. The soils are considered to be 16.5 m deep to bedrock, forming a single-layered, unconfined aquifer [*Campos and Freitas-Silva*, 1998].

7.1. Implementation of the Hydrologic Model

[43] The model was run using a digital elevation model (DEM) with 30 m grid spacing. Vertically the model was discretized in 10 layers of variable depths. The first layer is 0.5 m deep, the next two layers are 1 m deep, and the remaining seven layers are 2 m deep. The channel is composed of a single reach with 154 segments 30 m long each. Each segment is 4 m wide and 2.5 m deep. The hydrologic model assumes soils with 0.52 porosity, 0.24 volumetric residual water content, 0.37 volumetric soil moisture at field capacity, and 0.29 volumetric soil moisture at wilting point. The assigned horizontal hydraulic conductivity was 0.037 m h^{-1}, and the vertical hydraulic conductivity was 0.0037 m h^{-1}.

[44] Five reservoirs are built at different points, but only two reservoirs supply water for irrigation (Figure 2). Reservoir 2 has a maximum storage capacity of about 2400 m^3, and reservoir 5 has a maximum capacity of about 1800 m^3. Groundwater is used only for irrigation of gardens and groves in small properties within the community of farmers (farmer 4). A field of 24 wells is set within the community (Figure 2). The assigned proportion of groundwater extraction for irrigation is equally distributed between the 24 wells. Note that this does not mean that all wells can sustain the same amount of groundwater extraction (which depends on the depth and location of the well). The hydrologic model will indicate if any of the wells fails to produce the prescribed water. In that case, a new more restrictive groundwater availability constraint will be imposed in the next model iteration.

7.2. Implementation of the Economic Model

[45] Regarding socioeconomic characteristics, the Buriti Vermelho subcatchment area is a small watershed composed

Table 2. Farm Water Sources and Products[a]

Activity	Water Source	Irrigation Technology
	Large-Scale (Farm 1)	
Irrigated corn	adjacent watershed	center pivot
Rain-fed corn		
Irrigated beans	adjacent watershed	center pivot
Irrigated wheat	adjacent watershed	center pivot
Rain-fed sorghum		
Rain-fed soybeans		
	Large-Scale (Farm 2)	
Rain-fed corn		
Irrigated beans	reservoir 5	center pivot
Irrigated wheat	reservoir 5	center pivot
Rain-fed soybeans		
	Medium-Scale (Farm 3)	
Irrigated corn	reservoir 2	sprinklers
Irrigated beans	reservoir 2	sprinklers
Irrigated limes	reservoir 2	sprinklers
Irrigated vegetables	reservoir 2	drip
Irrigated orchard crops	reservoir 2	sprinklers
Rain-fed pasture		
Rain-fed soybeans		
	Small-Scale (Farm 4)	
Irrigated limes	reservoir 2 and well field	sprinklers
Irrigated vegetables	reservoir 2 and well field	sprinklers
Irrigated orchard crops	reservoir 2 and well field	sprinklers
Rain-fed pasture		

[a]Source, University of California, Davis/Embrapa field data.

of several types and scales of farming activities. Circles in Figure 2 identify the location and size of capital-intensive center-pivot irrigation schemes. Large patches of rain-fed agriculture remain in the Buriti Vermelho as the areas outside the center pivots for farmers 1 and 2. The tube well field is operated by an ensemble of small-scale farmers, which are grouped as farmer 4. The reservoirs from which farmers withdraw surface water are labeled.

[46] We identify four archetypical farm scales (see Table 2). Farms 1 and 2 are large-scale grain farms using center-pivot irrigation technology. Farm 3 can be viewed as a medium-scale operation with a diverse product mix. Farm 4 is a collection of homogeneous small-scale operations, each composed of multiple crops grown on about 3.8 ha each. Most of the descriptive data in this demonstration appear in Table 3. Data on the quantities of other inputs such as fertilizers, pesticides, and electricity were omitted for the sake of clarity. Farmers (of all scales of operation) in the Buriti Vermelho are assumed to be price takers. There is currently no market for water.

7.3. Baseline and Drought Scenarios

[47] On the hydrology side, a calibration run using rainfall and potential evapotranspiration data for the 2005 agricultural year is set as the baseline reference scenario as listed in Table 2. Water supply from the center pivots used by farmer 1 is imported from the adjacent basin, and it is assumed that the external source can satisfy the demand of the farmer (irrigation activity by farmer 1 is not constrained by water availability within the catchment area being modeled). Farmer 2 pumps water from reservoir 5 to supply water to the only center pivot situated near the basin outlet. Farmers 3 and 4 divert surface water from reservoir 2. In addition, farmer 4 has access to the well field to irrigate their small properties. The groundwater demand by farm 4 is divided homogeneously across the 24 wells. There are no water rights in place; farmers withdraw water from the sources to satisfy the demand that maximizes their net revenues given the physical and resource constraints.

[48] On the economic side, a calibration run was performed with the baseline data in Table 3 (plus the data, by crop and farmer, on other input quantities: fertilizers, pesticides, seeds, machinery, electricity used in irrigation, and

Table 3. Selected Baseline Values of Agricultural and Water Use Characteristics, by Farm Type

Farm Type and Agricultural Activity	Planted Area (ha)	Yield (tons/ha^{-1} or heads ha^{-1})	Total Annual Net Revenue (1000 Brazilian Reais)	Hired Labor Use (person-day ha^{-1})	Water Use (m^3 ha^{-1} yr^{-1})	
					Surface Water	Groundwater
			Large-Scale (Farm 1)			
Irrigated corn	157	9.0	141.7	0.9	3358	0
Rain-fed corn	126	5.5	68.1	0.2	0	
Irrigated beans	157	3.0	224.5	1.1	584	0
Irrigated wheat	86	5.5	72.9	0.9	4270	0
Rain-fed sorghum	80	3.6	30.2	0.2	0	0
Rain-fed soybeans	206	3.6	145.9	1.0	0	0
			Large-Scale (Farm 2)			
Rain-fed corn	314	4.5	128.7	0.2	0	0
Irrigated beans	42	2.9	32.9	1.1	1572	0
Irrigated wheat	20	4.9	15.8	1.8	4282	0
Rain-fed soybeans	318	3.1	168.7	1.5	0	0
			Medium-Scale (Farm 3)			
Irrigated corn	4	7.5	2.1	1.6	2300	0
Irrigated beans	4	2.8	2.9	2.6	1806	0
Irrigated limes	3	11.2	5.3	7.4	3200	0
Irrigated vegetables	9	20.0	56.5	16.2	2670	0
Irrigated orchards	3	14.0	13.0	18.3	3000	0
Rain-fed pasture	2	2.0	0.8	2.0	0	0
Rain-fed soybeans	4	2.9	1.5	0.8	0	0
			Small-Scale (Farm 4)			
Irrigated limes	28	14.0	118.5	7.4	2662	0
Irrigated vegetables	37	16.0	158.9	3.8	3857	0
Irrigated orchards	19	10.8	61.9	14.5	4014	0
Rain-fed pasture	10	15.0	52.3	5.1	0	0

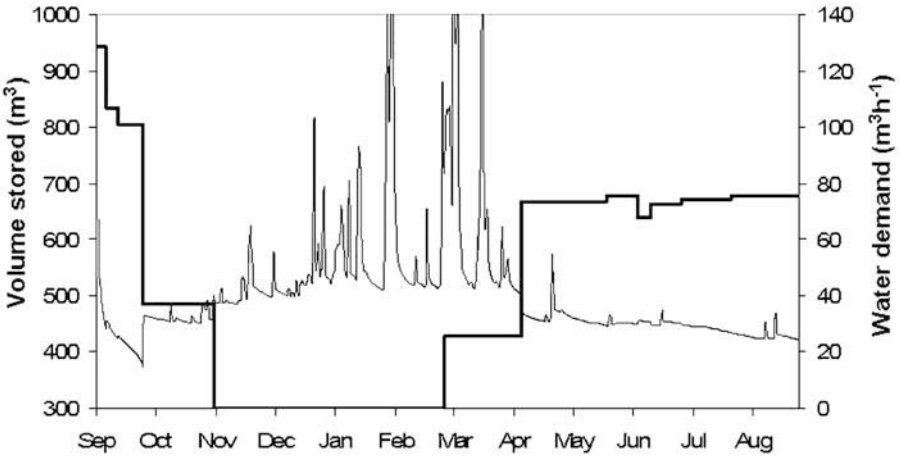

Figure 3. Calculated water storage (thin curve) and water diversions (bold curve) from reservoir 2 for the baseline simulation. The large fluctuations in storage are due to the small size of the reservoir with respect to the inflows. Reservoirs in the study area were built to maintain the water levels above the diversion channel and not to store water.

irrigation capital). Using these data, parameter values for the rain-fed and irrigated crops production functions were calculated and introduced to equations (4) and (5). The parameterized production functions were then used in the model set up by equations (13) and (14). The results from this optimization run in terms of crop and input mix, including surface and groundwater use, were then verified against the baseline values. Ninety-two percent of the differences between what the model predicts and the baseline data were within an acceptable range between 0% and 4%. In this fashion, the economic model was then considered as calibrated.

[49] In order to assess the response of the hydrologic and of the economic systems two more optimization runs were done simulating droughts of different severities with respect to the baseline case. In the drought scenarios, all is kept identical as the baseline except for 25% and 50% reduction in precipitation and 15% and 25% increase in evapotranspiration for drought scenarios 1 and 2, respectively. The exercise is intended as a sensitivity analysis to test the models and give guidance to drought policy making.

[50] Finally, it is worth noting that the effect of the elasticity of substitution parameter on the results was evaluated. A sensitivity analysis was run using elasticity of substitution parameter values ranging from 0.25 to 0.8. This analysis showed that in this range there is little variation in the outputs and thus does not carry into the results presented below.

8. Results

8.1. Baseline Scenario

[51] After running the model for the baseline scenario, surface water was not binding for farmers, so there was no need to resort to groundwater for irrigation. Farmers 3 and 4 withdrew water from reservoir 2. The evolution of the storage in this reservoir and the rate at which water is diverted (demand) is shown in Figure 3. The most intense diversions from the reservoir were at the beginning of the simulation period, which is the end of the dry season. There is one short pulse of water demand of about 128 $m^3 h^{-1}$ that soon drops to about 101 $m^3 h^{-1}$ and then further to about 37 $m^3 h^{-1}$. Those water withdrawals correspond to irrigation of the last stages of crops planted the previous season that gradually decrease as the crops are harvested. By November, the wet season has begun and crop water requirements were satisfied by incident rainfall, but by early March and until April the decrease in precipitation made some supplemental irrigation necessary.

[52] As the dry season advanced the demand for irrigation increased to an average constant requirement of about 74 $m^3 h^{-1}$ from mid-April through the end of the season. Farmer 2 supplied water to the center pivot from reservoir number 5 (Figure 4). The pivot irrigated the last stages of crops planted at the end of the dry period the previous season causing a demand peak of over 90 $m^3 h^{-1}$ for a short period. Farmer 2 started irrigation at a demand rate of 57 $m^3 h^{-1}$ again in late March when he grows beans, although water requirements decreased between 20 and 30 $m^3 h^{-1}$ later in the dry season when he grows wheat. The inflows to both reservoirs were typically larger than the water demands so a decline in the storage is only clearly noticeable during very high demand peaks (recovery of storage when high demand loads at the beginning of the simulation period decrease). Therefore, because surface water was not binding to farmers, no groundwater was extracted for irrigation.

[53] The results of the baseline for crop mix, irrigated areas, yield, net revenues, labor use, applied water, and water productivity is shown in Table 3. Farms 1 and 2 are large-scale farms with large rain-fed areas and center pivots to irrigate corn, dry beans, and wheat. Farm 1 irrigated 157 out of the 283 ha of corn planted (total size of the center pivot) and 157 ha of beans. Irrigated corn and irrigated beans were their most profitable crops. Dried beans along with rain-fed soybeans were the most labor demanding crops. Farm 2 did not irrigate corn but irrigated all the beans and wheat planted under the small center pivot. Rain-fed corn and irrigated beans were the most profitable crops. Farmer 3 is a more diversified farmer and irrigated all crops except pasture and soybeans. Vegetables and orchard crops were most profitable but also the most labor intensive. Farmer 4 is a set of small-

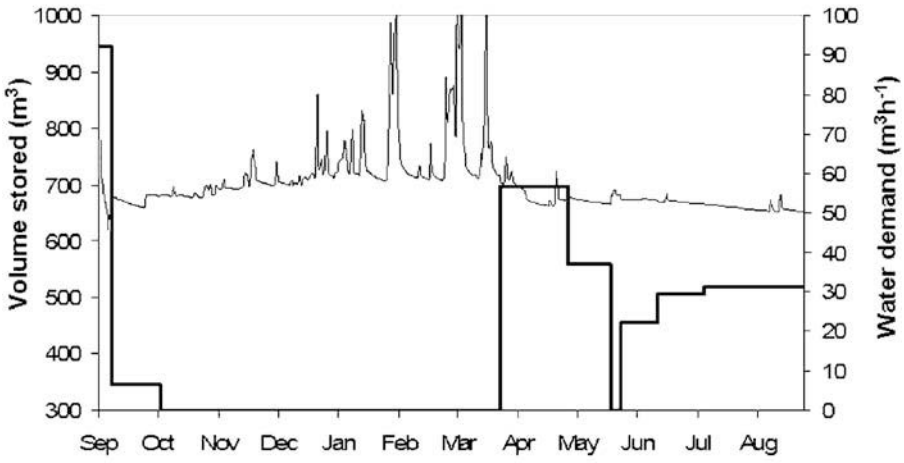

Figure 4. Calculated water storage (thin curve) and water diversions (bold curve) from reservoir 5 for the baseline simulation. The large fluctuations in storage are due to the small size of the reservoir with respect to the inflows. Reservoirs in the study area were built to maintain the water levels above the diversion channel and not for water storage.

scale producers with small irrigated plots. They irrigated all products except pasture. Vegetables and limes were the most profitable crop.

8.2. Drought Scenarios

[54] The water available for irrigation in the basin is strongly influenced by the decrease in precipitation and increase in atmospheric demand set in the drought scenarios. The effects of the drought are not the same for all farmers and at all times. There is a strong spatial and temporal component in the availability of water and in its demand. Figure 5 shows the evolution of the water storage and the change in water diverted from reservoir 2 for the two drought scenarios run in the simulation. The reduction in inflows to the reservoir for drought scenario 1 forces farmer to react, which is reflected in reduced water diversions respect to the baseline scenario. Still, the reductions are small (between 2% and 9% with respect to the baseline), indicating that water is not strongly binding. In fact, there is about a 2% increase in the water diverted from the reservoir between September and October with respect to the baseline case to partially compensate for the rainfall shortfalls.

[55] For the other more severe drought scenario, the impact on the inflows to the reservoir and on the reservoir storage was enough to make surface water strongly binding to farmers during the entire year. Still, irrigation during the wet

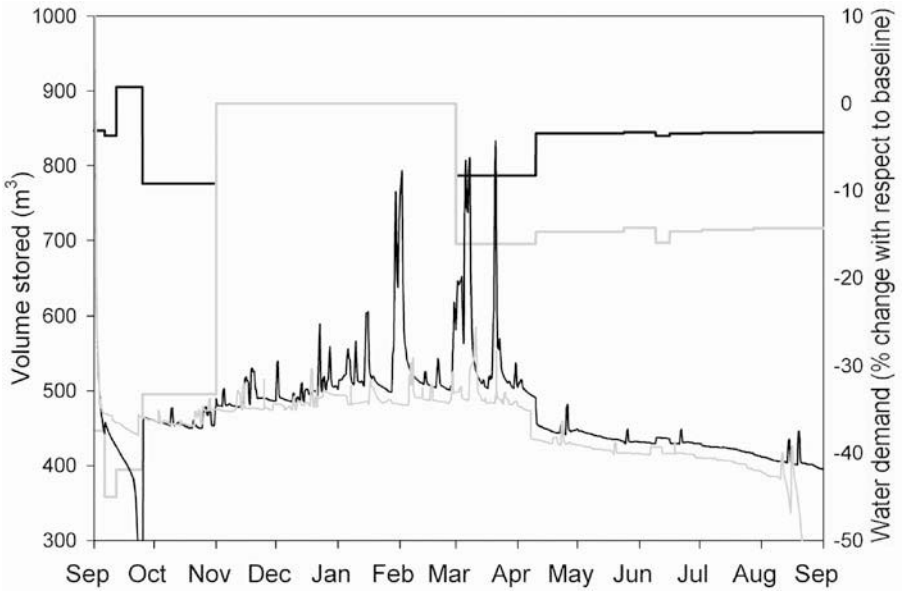

Figure 5. Calculated water storage (thin curves) and change in water diversions from reservoir 2 with respect to the baseline simulation (bold curves) for the 25% precipitation reduction (black lines) and the 50% precipitation reduction (gray lines) scenarios. The large fluctuations in storage are due to the small size of the reservoir with respect to the inflows. Reservoirs in the study area were built to maintain the water levels above the diversion channel and not for water storage.

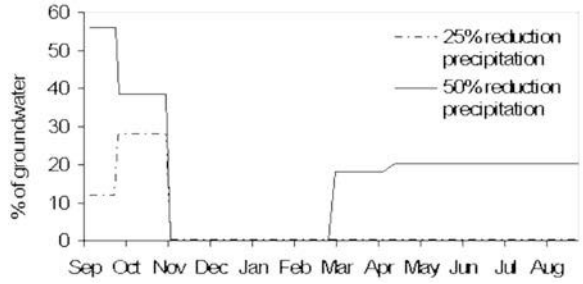

Figure 6. Proportion of groundwater in total applied water by farm 4 for the two drought scenarios.

season was not necessary. In many months farmers drew water from the reservoir at the maximum rate allowed by inflows (the reservoirs are small and are only used to minimize fluctuations in the elevation of the water surface to ensure a steady hydraulic head and not as an effective water storage). In the severe drought scenario, water became the main limiting factor for agricultural productivity and farmers maximized the use of water and finished the year with an empty reservoir.

[56] Overall, a reduction of 25% in precipitation forced a reduction of diverted water from the reservoir an average of 3% with peak reductions of 9% with respect to the amounts of water diverted the baseline year. A 50% precipitation shortfall reduced diversions an average of 13% although those reductions were as high as 45% at the beginning of the simulation period. Because water became a limiting factor for productivity during the droughts, pumping groundwater started to be profitable for farm 4. Figure 6 shows the proportion of applied water from groundwater for farm 4. For a 25% reduction in precipitation a supplement of groundwater (12–29% of total applied water) was only necessary to finish the crops at the end of the dry season. For the 50% reductions in precipitation, groundwater proportions of total applied water by farm 4 increased between 40% and 55% from September to November.

[57] After the wet season, ~16% of applied water was from groundwater. The groundwater supplements were smaller at the end of the period compared with the rate at which groundwater was pumped at the beginning because a larger amount of water was required (longer irrigation period after the wet season) and the groundwater table elevation did not recover compared with the baseline initial depth, and therefore its pumping cost remained high as the season advanced (Figure 7). It should be kept in mind that the drought scenarios have a reduction in precipitation and an associated increase in atmospheric demand, which increases water consumption by plants, accelerates evaporation from reservoirs, and reduces groundwater recharge.

[58] The water diversion operations in reservoir 2 strongly affected reservoir 5 and the behavior of farm 2 (Figure 8). With 25% reduction in precipitation, farm 2 increased irrigation when possible to make up for the rain shortfall. In this scenario farm 2 diverted ~25% more surface water to increase irrigation at the end of the wet season, when water was still available, to compensate for the reduced rainfall and for the loss of productivity in rain-fed crops. As the dry season continued, the intensification of diversions from reservoir 2 reduced the water inflows to reservoir 5, forcing farm 2 to reduce irrigation to almost 40% of the water diverted in the baseline scenario. For the more severe 50% rainfall reduction drought scenario, water availability in reservoir 5 became more restricted and farm 2 lost the opportunity of increasing irrigation even for a short period at the end of the wet season. Unlike the 25% precipitation reduction scenario, water diversion at the end of the wet season for the 50% rain shortfall was reduced almost 20% with respect to the baseline amount. Later in the dry season, as water became even less available because of the drought and the intensified water use upstream, the water diverted from the reservoir was severely reduced to 65% of the baseline amounts.

[59] In general, farmers reacted to reduced rainfall by decreasing the applied water per hectare and therefore stressing the crops and accepting productivity losses. The sharpest reduction in applied water was by farm 2 for wheat (Figure 9). Farmer 2 is at the end of the river channel drawing water from reservoir 5, which receives the remnant water once the other farmers have withdrawn water from reservoir 2 located upstream.

[60] Farm 3 had a small total irrigated area and withdrew water from reservoir 2 having maximum accessibility to the available surface water and so did not significantly stress the crops but rather increased the amount of supplemental irrigation for corn, limes, and vegetables to compensate for decreased precipitation. The lower levels in reservoir 2 had a larger effect on farm 4 because his total irrigated area is larger than for farm 3 and therefore required more water. Even though farm 4 had access to groundwater, farm 4 still reduced applied water per hectare for vegetables and fruits.

[61] Farmers also reacted by changing the cropped areas for the products they grow (Figure 10). For each drought scenario, the area planted with rain-fed crops (e.g., pasture, soybeans, and sorghum) was either sharply reduced (e.g., pasture for farm 3 or 4 or soybeans for farms 2, 3, and 4 for drought scenario 1) or totally eliminated (pasture for farm 4, drought scenario 2). Typically those reductions in rain-fed crops were compensated by increasing the areas dedicated to irrigated crops. This reshuffling of crop mix in response to water scarcity is a result of the nonuniform marginal contribution of water to farm level profitability and to the farmer's effort to allocate the increasingly scarce water to the most profitable crops at the different periods of the year.

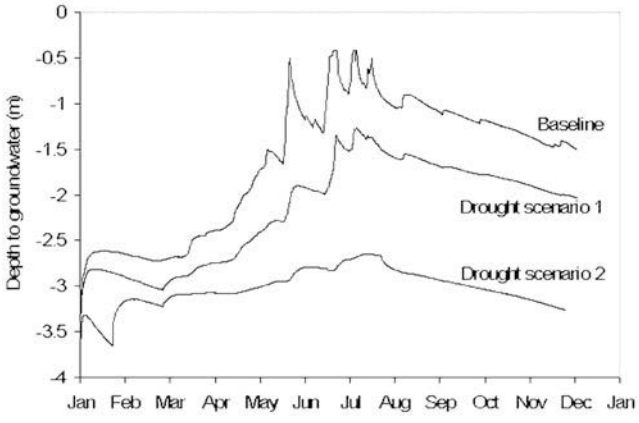

Figure 7. Depth to the water table in one of the wells used by farm 4.

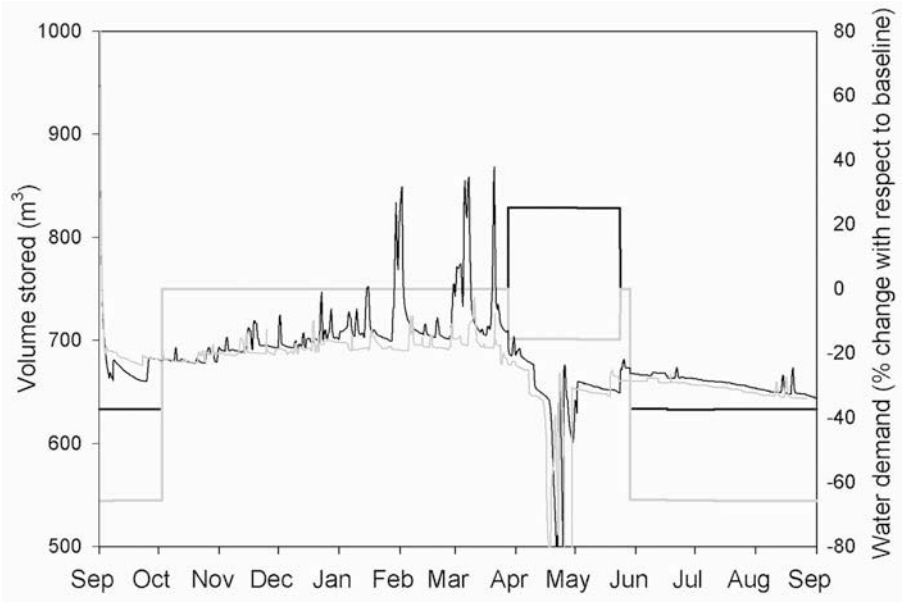

Figure 8. Calculated water storage in (thin curves) and change in water diversions from reservoir 5 with respect to the baseline case (bold curves) for the 25% precipitation reduction (black lines) and 50%.

[62] As indicated by hydrologic results, farmers' reactions and their location relative to the resources had effects on the amount of water they could use for irrigation. Farm 3 withdraws water from the upstream end of the system (reservoir 2) and therefore had the best opportunity for surface water use. That farm reacted to the decrease in precipitation by reducing the area planted with rain-fed crops (pasture and soybeans) and increasing irrigation in his irrigated products, which resulted in an increase use of water with respect to the baseline values (Table 4). The negative impact of farm 3's

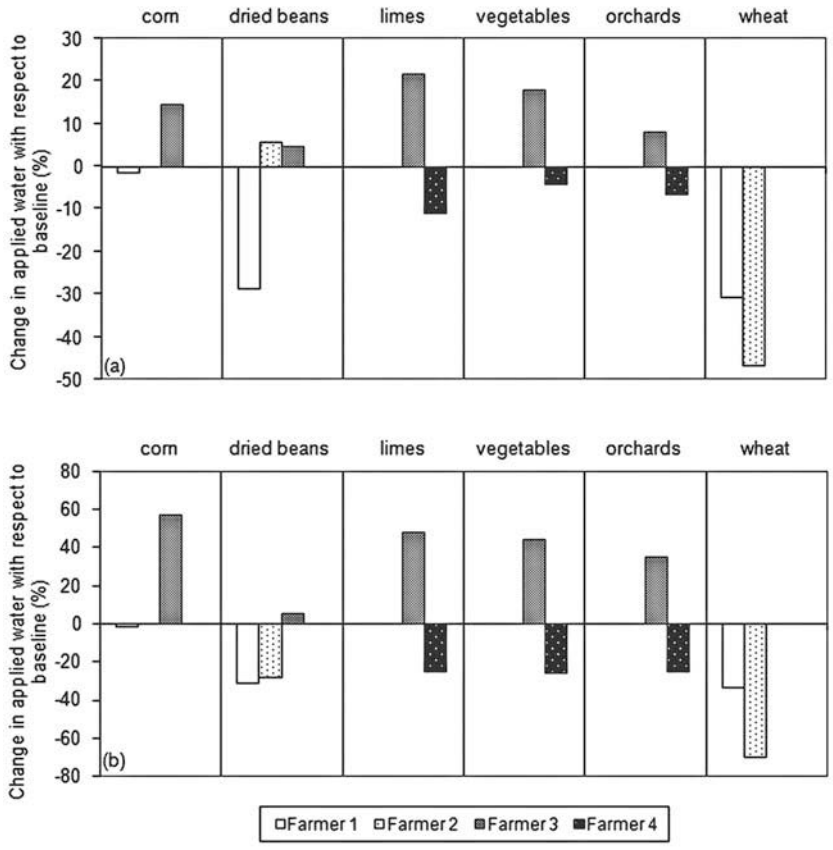

Figure 9. Changes in applied water for the irrigated crops with respect to baseline applied water: (a) 25% precipitation reduction scenario and (b) 50% precipitation reduction scenario.

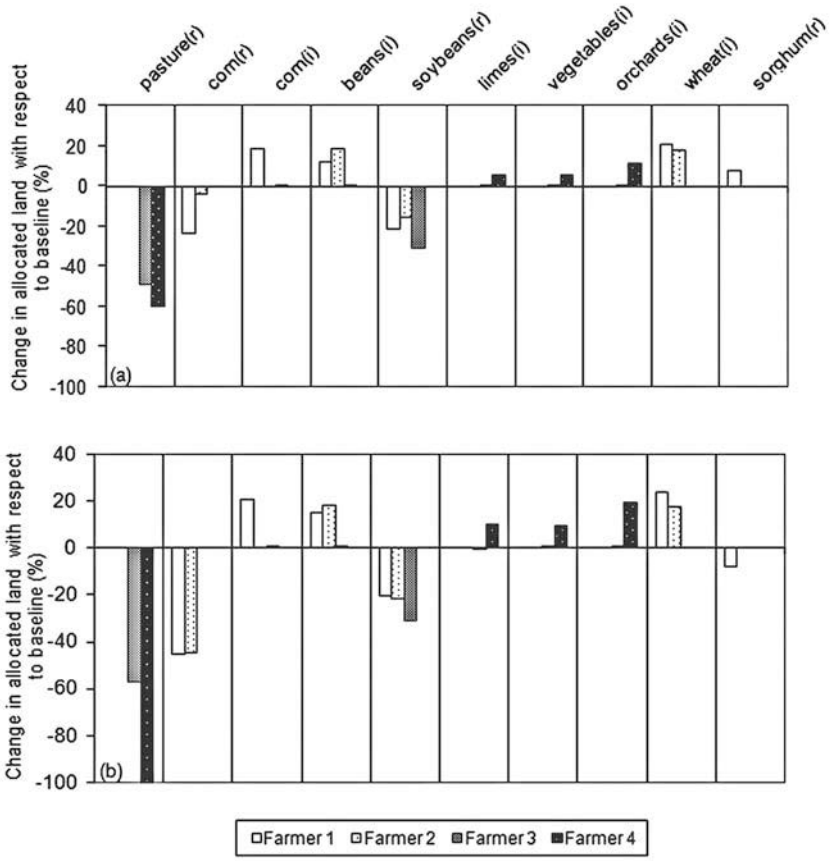

Figure 10. Changes in allocated land per crop with respect to baseline areas: (a) 25% precipitation reduction scenario and (b) 50% precipitation reduction scenario. Letter "r" indicates rain-fed, and "i" indicates irrigated.

decisions on farm 2 forced the latter to increase the stress on the irrigated crops and to reduce the areas dedicated to them. Farmer 4 avoids a decrease in crop production by increasing groundwater use.

[63] Crop diversification, total applied water, and access to different water sources also explain a large part of the variation of farm profits in the event of a drought. Table 5 shows the changes in farm profits (from the baseline reference) for the different drought scenarios, and Figure 11 shows the change in profit per farmer and per crop. Farm 1 and farm 2 are the largest but least diversified (only grain) farmers, and they had the largest rain-fed areas (planted with corn, soybeans, and sorghum); therefore the decrease in rainfall had a strong impact in their net revenues. On the other hand, farm 3 had few rain-fed crops, is located upstream and hence had first access to surface water, and is well diversified (grains, orchard crops, vegetables, and pasture). This greatly reduced the effect of droughts on overall profitability. Farm 4 mitigated the effects of the drought by resorting to groundwater extraction. Although profits for this farm decreased 6.8% and 8.6% for the drought scenarios 1 and 2, respectively (Table 4), without access to groundwater the impacts on profits from reduced precipitation would have been much greater.

[64] Farmers not only adjust crop area and applied water in dry years, but they also adjust other inputs that may affect productivity and farm profitability. For instance, hired labor was also very sensitive to reduced rainfall and may have an external impact on the local economy. In Figure 12 it can be seen that hired labor was reduced for rain-fed crops and eliminated for pasture (farm 3 and farm 4) and soybeans (farms 1, 2, and 3) when farmers eliminated those crops in

Table 4. Percent Change in Applied Water per Source per Farm With Respect to Baseline Applied Water, by Drought Scenario, by Farm Type

	Scenario 1	Scenario 2
Farm 1	1	1.1
Farm 2	−10	−43.8
Farm 3	15	42
Farm 4, surface water/groundwater	−5/+6	−27.2/40

Table 5. Change in Total Farm Profits per Year With Respect to the Baseline Scenario, by Drought Scenario, by Farm Type

	Scenario 1	Scenario 2
Farm 1	−17.1	−19.9
Farm 2	−48.0	−62.3
Farm 3	−1.3	−1.4
Farm 4	−6.8	−8.6

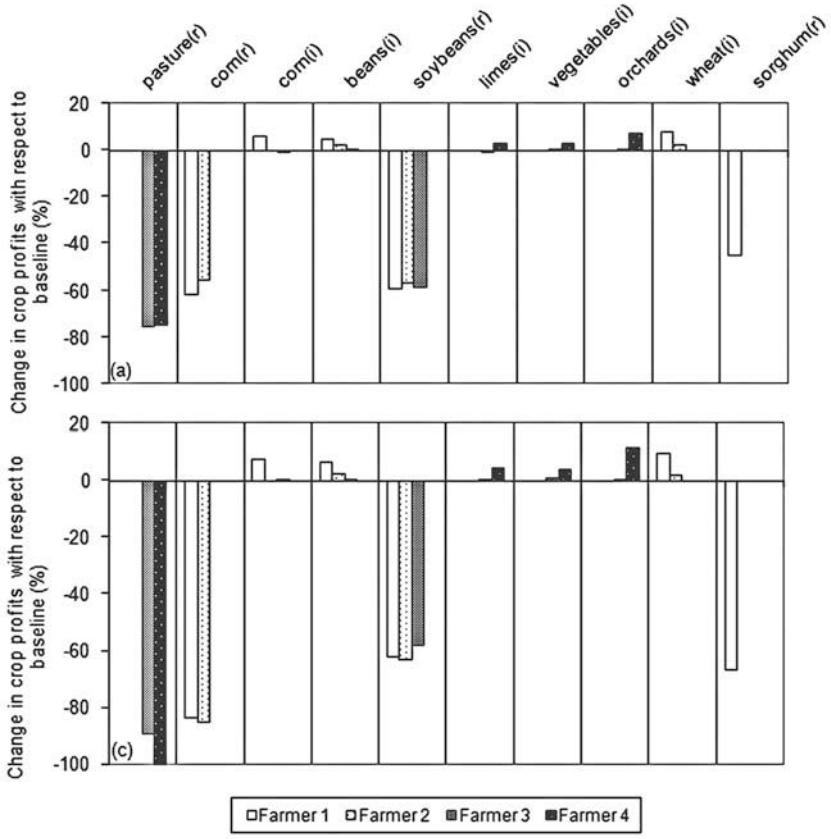

Figure 11. Changes in crop-specific profits with respect to baseline values: (a) 25% precipitation reduction scenario and (b) 50% precipitation reduction scenario. Letter "r" indicates rain-fed, and "i" indicates irrigated.

drought scenario 2. For drought scenario 2, hired labor was severely cut back for corn and wheat (farm 2).

[65] Whenever possible, farmers will try to improve yield by increasing labor in their most profitable crops such as dried beans (farm 3) or corn and wheat (farm 1) as a substitute for water. Because the constant and common elasticity of substitution, unconstrained inputs (fertilizers, pesticides, seeds, and machinery) have the same magnitude of change so they can be pooled together as materials and machinery. Table 6 shows the changes in total quantities of those inputs for the crops most affected by the most severe scenario by farm 2 and farm 4. Again, farmers reduced materials and machinery for the rain-fed crops but increased them for his irrigated crops in an attempt to maintain net revenues by reallocating costs in materials and machinery to their most profitable crops.

9. Discussion

[66] The results show how severe reductions in the amount of precipitation force farmers to change product and input mix. Furthermore, the reduction in net revenues is not proportional to the precipitation cutbacks. Water management adaptations that significantly mitigate the impact of dry warming scenarios and that include more conjunctive subsurface-surface water use were also found for large multisectorial systems such as the Central Valley of California [*Medellín-Azuara et al.*, 2008; *Tanaka et al.*, 2006]. In systems investigated in this research, the strategy that farmers follow to deal with decreased rainfall depends largely on their location within the basin. For severe reductions in precipitation, farmers located upstream with better access to water will replace their rain-fed crops with irrigated products increasing their amount of used water. Farmers located downstream will be affected not only by a reduction in precipitation but also by a reduction in their inflows due to the upstream intensification of the irrigation activity. In the absence of water rules, farmers located downstream will stress irrigate their crops and will be affected the most in the event of a drought while allocating the available water to higher valued crops as also reported by *Cai* [2008], thus increasing its marginal value. In the absence of surface water (at no charge in the study area), farmers with wells start finding it profitable to pump more groundwater to supplement irrigation although the depth to the water table and thus pumping costs increase during a period of drought and during the months when the water is needed most (the unitary cost of groundwater (p_{gw}) for the 50% precipitation reduction scenario ranges from 0.37 cents of Brazilian Reais in April to 0.44 cents in August). For this, farmers allocate water to high-value, drought-sensitive products. Farmers with access to groundwater will reduce the risk of losing crops to a drought but will only turn to that source when cheaper surface water becomes scarce or expensive as also reported in other studies [*Lefkoff and Gorelick*, 1990b; *Schoups et al.*, 2006]. For several drought-tolerant products, farmers may stress irrigate

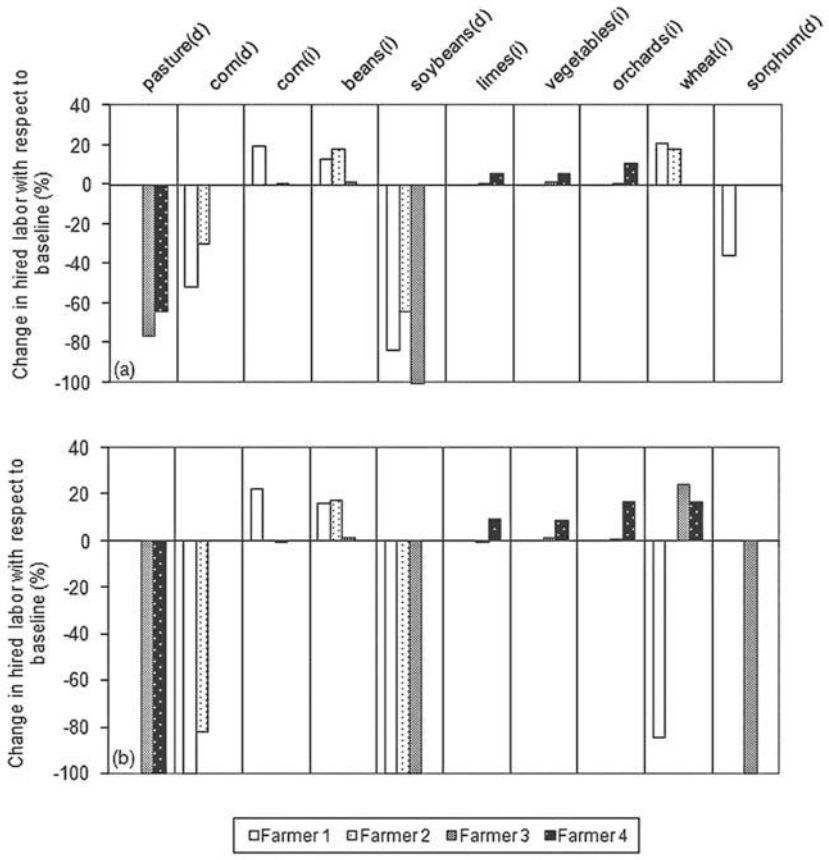

Figure 12. Changes in hired labor dedicated per crop with respect to the baseline hired labor: (a) 25% precipitation reduction scenario, and (b) 50% precipitation reduction scenario. Letter "r" indicates rain-fed, and "i" indicates irrigated.

the crops and keep the planted area large rather than reduce the area and provide the crop with optimal irrigation. It is worth nothing that the final optimal solutions would be more optimistic if the spatial distribution of groundwater had not been taken into account. During our optimization runs, farm 4 had to scale back its crops because wells located in some points would run out of water or had to decrease the diversion rates from wells that had lower recharge rates.

[67] In terms of timing of effects, in case of a severe drought water diversion is the highest at the end of the summer, when supplemental water is needed to complete a large area of high demanding crops planted at the end of the rainy season. Groundwater use slightly increases after the rainy season when surface water becomes scarce. Few models in the literature optimize intraseasonal water application. *Cai et al.* [2003a] and *Cai* [2008] offered a formulation that used monthly intervals to calculate restrictions to the economic model and indicate that without the optimization at a temporal resolution higher than a season, erroneous groundwater pumping or reservoir releases will be calculated.

Table 6. Changes in Total Use of Fertilizers, Pesticides, Seeds, and Machinery With Respect to the Baseline Scenario, for Farm 2 and Farm 4

	Materials and Machinery	
Crop	25%	50%
Farm 2		
Rain-fed corn	−30.3	−82.1
Irrigated beans	18.2	17.4
Rain-fed soybeans	−63.8	−100
Irrigated wheat	17.8	16.9
Farm 4		
Irrigated limes	5.6	9.2
Irrigated vegetables	5.2	8.5
Irrigated orchards	10.4	16.6
Rain-fed pasture	−64.3	−100

10. Conclusions

[68] A hydroeconomic model has been presented linking a 3-D spatially distributed and physics-based hydrologic model, and an economic model of agriculture based on a nonlinear multi-input multioutput production function, solved using positive mathematical programming. The model was applied to an experimental watershed in Brazil to test its capabilities and investigate the economic behavior of farmers, the agricultural production, and the interactions between the hydrologic and the agricultural systems.

[69] In the present study, the hydrologic component takes into account the spatial distribution of water within the landscape with high resolution and therefore ensures convergence to a solution that is hydrologically feasible at all points in the landscape. The high resolution also permits calculating water restrictions at the farm level allowing the use of farm

resolution economic information. Given the differences in crop types and irrigation technology, an aggregation by district or region as seen in other models would have very different economic and hydrologic response functions to changes. Aggregate efficiency measures gloss over distributional impacts of water policy changes.

[70] Also, the presented approach explicitly includes effective precipitation as an argument in the production function within a positive mathematical programming framework. The models are linked at a monthly time step, so intraseasonal water application can be optimized even though the production function technically works at the season scale. Herein, the higher resolution of the hydroeconomic linking permits more detailed insight into the temporal distribution of the water requirements within the season taking into account the different crop growth stages and within-season fluctuation of water availability (using also monthly restrictions to the economic system).

[71] Future work may involve implementing an uncertainty component to the model and a risk aversion component to the model that will optimize input and product mix. This is especially important in semiarid areas or areas of high variability of precipitation or in environments with variable commodity prices.

Appendix A: Analytical Calculation of the Production Function Parameters

[72] In this example we consider the estimation of the production function parameters for irrigated crops (the same methodology can be used for the estimation of the parameters of the production function for rain-fed crops). We demonstrate the method for 4 inputs: land (*land*), surface water (*sw*), groundwater (*gw*), and hired labor (*lb*). The method can be easily expanded for all inputs used in equation (5).

[73] A CES production function with these 4 inputs is

$$q_i = A_i\left[b_{i\,lb}X_{i\,lb}^{\gamma} + b_{i\,land}X_{i\,land}^{\gamma} + b_{i\,w}\ X_{i\,sw} + X_{i\,gw} + P_i\right)^{\gamma}\Big]^{\frac{1}{\gamma}}, \quad \text{(A1)}$$

letting uX be an alias for the function inside the brackets. Taking the derivative of equation (A1) with respect to X_{ifl}, we obtain

$$\frac{\partial q_i}{\partial X_{i\,land}} = \gamma b_{i\,land}X_{i\,land}^{\gamma-1}\frac{1}{\gamma}A_i(uX)^{\frac{1}{\gamma}-1}. \quad \text{(A2)}$$

Also since $\gamma = (\sigma - 1)/\sigma$ (see section 2.2)

$$\gamma - 1 = \frac{1}{-\sigma} \quad \text{(A3)}$$

$$\frac{1}{\gamma} - 1 = \frac{1}{\sigma - 1}, \quad \text{(A4)}$$

substituting equation (A3) and equation (A4) into equation (A2), we obtain

$$\frac{\partial q_i}{\partial X_{i\,land}} = b_{i\,land}X_{i\,land}^{-\frac{1}{\sigma}}A_i(uX)^{\frac{1}{\sigma-1}}. \quad \text{(A5)}$$

[74] By following these same steps for the other inputs, we get

$$\frac{\partial q_i}{\partial X_{i\,lb}} = b_{i\,lb}X_{i\,lb}^{-\frac{1}{\sigma}}A_i(uX)^{\frac{1}{\sigma-1}} \quad \text{(A6)}$$

$$\frac{\partial q_i}{\partial X_{i\,sw}} = b_{i\,w}\ X_{i\,sw} + X_{i\,gw} + P_i\ )^{-\frac{1}{\sigma}}A_i(uX)^{\frac{1}{\sigma-1}}. \quad \text{(A7)}$$

Notice in equation (A7) that we have used surface water to calculate the marginal productivity of water. In fact, since it is assumed that there is no difference in surface water, groundwater, or precipitation quality, the marginal impact of an extra unit of water (from any source) has the same effect on production. Only surface and groundwater are under control of the farmer and surface water was chosen to calculate the optimality condition because in our baseline scenario, which represents the real conditions in the field at the time of the survey, no crops were irrigated using groundwater.

[75] By equating the value of the marginal product in crop i for each input with their respective marginal cost (market prices plus shadow values), we get

$$VMP_{i\,lb} = p_i\frac{\partial q_i}{\partial X_{i\,lb}} = p_i b_{i\,lb}X_{i\,lb}^{-\frac{1}{\sigma}}A_i(uX)^{\frac{1}{\sigma-1}} = p_{lb} \quad \text{(A8)}$$

$$\begin{aligned} VMP_{i\,land} &= p_i\frac{\partial q_i}{\partial X_{i\,land}} = p_i b_{i\,land}X_{i\,land}^{-\frac{1}{\sigma}}A_i(uX)^{\frac{1}{\sigma-1}} \\ &= p_{land} + \lambda_{land} + \lambda_{i\overline{land}} \end{aligned} \quad \text{(A9)}$$

$$\begin{aligned} VMP_{i\,sw} &= p_i\frac{\partial q_i}{\partial X_{i\,sw}} = p_i b_{i\,sw}\ X_{i\,sw} + X_{i\,gw} + P_i\ )^{-\frac{1}{\sigma}}A_i(uX)^{\frac{1}{\sigma-1}} \\ &= p_{sw} + \lambda_{sw}. \end{aligned} \quad \text{(A10)}$$

From equation (A8) and equation (A9), we get

$$\frac{b_{i\,lb}X_{i\,lb}^{-\frac{1}{\sigma}}}{b_{i\,land}X_{i\,land}^{-\frac{1}{\sigma}}} = \frac{p_{lb}}{p_{land} + \lambda_{land} + \lambda_{i\overline{land}}}$$

or

$$b_{i\,land} = b_{i\,lb}\frac{p_{land} + \lambda_{land} + \lambda_{i\overline{land}}}{p_{lb}}\left(\frac{X_{i\,lb}}{X_{i\,land}}\right)^{-\frac{1}{\sigma}}. \quad \text{(A11)}$$

Likewise, from equations (A8) and (A10),

$$b_{i\,w} = b_{i\,lb}\frac{p_{sw} + \lambda_{sw}}{p_{lb}}\left(\frac{X_{i\,lb}}{X_{i\,sw} + X_{i\,gw} + P_i}\right)^{-\frac{1}{\sigma}}. \quad \text{(A12)}$$

The constant returns to scale assumption implies that

$$b_{i\,lb} + b_{i\,land} + b_{i\,w} = 1, \quad \text{or} \quad b_{i\,lb} = 1 - b_{i\,land} - b_{i\,w}. \quad \text{(A13)}$$

[76] Substituting equations (A11) and (A12) in (A13), we have

$$b_{ilb} = 1 - b_{il}\frac{p_{land} + \lambda_{land} + \lambda_{iland}}{p_{lb}}\left(\frac{X_{ilb}}{X_{iland}}\right)^{-\frac{1}{\sigma}} - b_{il}\frac{p_{sw} + \lambda_{sw}}{p_l}\left(\frac{X_{il}}{X_{isw} + X_{isw} + P_i}\right)^{-\frac{1}{\sigma}} \quad \text{(A14)}$$

Dividing all terms of (A14) by b_{ilb} and solving for b_{ilb}, we obtain

$$\hat{b}_{ilb} = 1 + \frac{p_{land} + \lambda_{land} + \lambda_{iland}}{p_{lb}}\left(\frac{X_{ilb}}{X_{iland}}\right)^{-\frac{1}{\sigma}} + \frac{p_{sw} + \lambda_{sw}}{p_{lb}}\left(\frac{X_{ilb}}{X_{isw} + X_{igw} + P_i}\right)^{-\frac{1}{\sigma}}\Bigg)^{-1}. \quad \text{(A15)}$$

Substituting equation (A15) into equations (A11) and (A12), we get expressions for parameters $\hat{b}_{iland}$ and $\hat{b}_{iw}$. Parameters b can then be calculated by using data on input prices p_h and on input quantities X_{ih}, resource shadow values λ_{land}, λ_{sw}, the value on the Lagrange multiplier associated with the land calibration constraint λ_{iland}, and a value for the elasticity of substitution σ, which for this exercise is assumed to be equal to 0.25.

[77] Finally, by substituting their values back into equation (A1), and using the data on output quantity y_i associated with crop i, we obtain an estimate for the parameter A_i:

$$\hat{A}_i = \frac{q_i}{\left(\hat{b}_{ilb}X_{ilb}^{\gamma} + \hat{b}_{iland}X_{iland}^{\gamma} + \hat{b}_{iw}\ X_{isw} + X_{igw} + P_i\ \right)^{\frac{1}{\gamma}}}. \quad \text{(A16)}$$

Appendix B: Analytical Calculation of the Implicit Land Cost Function Parameters

[78] Departing from the standard definition of elasticity of supply for product i η_i, we have

$$\eta_i = \frac{\partial q_i}{\partial p_i}\frac{p_i}{q_i}. \quad \text{(B1)}$$

This equation measures the extent to which the supply of crop i increases given a marginal increase in its price p_i at a given point represented by price p_i and quantity q_i.

[79] The marginal cost of land (MC_i) is defined as the derivative with respect to land of the total cost of land associated to crop i (TCL_i), which is the sum of the implicit cost function and the per-unit cost of land, $TCL_i = \alpha_i X_{iland} + 0.5\psi_i X_{iland}^2 + p_{land}X_{iland}$:

$$MC_i = \alpha_i + \psi_i X_{iland} + p_{land}. \quad \text{(B2)}$$

Assuming perfect competition in which p_i equals the marginal cost of land MC_i and further assuming constant yield per hectare ($\hat{y}_i = q_i/X_{iland}$), then

$$MC_i = \alpha_i + \psi_i\frac{q_i}{\hat{y}_i} + p_{land} \quad \text{(B3)}$$

and $\partial q_i/\partial p_i$ in (B1) can be viewed as the inverse of the derivative of MC_i with respect to q_i, i.e.,

$$\left(\frac{\partial MC_i}{\partial q_i}\right)^{-1} = \frac{\hat{y}_i}{\psi_i}.$$

[80] In this manner equation (B1) can be rewritten as

$$\eta_i = \frac{\hat{y}_i}{\psi_i}\frac{p_i}{\hat{y}_i X_{iland}}, \quad \text{or} \quad \hat{\psi}_i = \frac{1}{\eta_i}\frac{p_i}{X_{iland}}. \quad \text{(B4)}$$

Therefore, with prior information on the elasticity of supply, assumed in this exercise to be 2.5 for all crops, plus information on output prices p_i and land allocation X_{iland}, we can calculate parameter $\hat{\psi}_i$.

[81] Now let the average cost of land (AC_i) be defined as TCL_i divided by X_{iland} and $AC_i = \alpha_i + 0.5\psi_i X_{iland} + p_{land}$. Data on AC_i can be obtained by subtracting the estimated average cost of each individual input except X_{iland} from the total average cost reported by the farmer. AC_i together with information on p_{land} and $\hat{\psi}_i$ calculated in (B4) is used to calculate parameter α_i:

$$\hat{\alpha}_i = AC_i - 0.5\hat{\psi}_i X_{iland} - p_{land}. \quad \text{(B5)}$$

[82] **Acknowledgments.** Financial support for this research has been provided in part by the CGIAR's Challenge Program on Water and Food, the Empresa Brasileira de Pesquisa Agropecuaria (Embrapa), and the Center for Natural Resources Policy Analysis, UC Davis.

References

Allen, R. G., L. S. Pereira, D. Raes, and M. Smith (1998), *Crop Evapotranspiration: Guidelines for Computing Crop Water Requirements*, 300 pp., Food and Agric. Organ. of the United Nations, Rome.

Brown, C., and P. Rogers (2006), Effect of forecast-based pricing on irrigated agriculture: A simulation, *J. Water Resour. Plann. Manage.*, *132*(6), 403–413, doi:10.1061/(ASCE)0733-9496(2006)132:6(403).

Brown, C., P. Rogers, and U. Lall (2006), Demand management of groundwater with monsoon forecasting, *Agric. Syst.*, *90*(1–3), 293–311, doi:10.1016/j.agsy.2006.01.003.

Burt, O. R. (1964), Optimal resource use over time with an application to ground water, *Manage. Sci.*, *11*(1), 80–93, doi:10.1287/mnsc.11.1.80.

Cai, X. (2008), Implementation of holistic water resources-economic optimization models for river basin management: Reflective experiences, *Environ. Modell. Software*, *23*(1), 2–18, doi:10.1016/j.envsoft.2007.03.005.

Cai, X., and D. Wang (2006), Calibrating holistic water resources-economic models, *J. Water Resour. Plann. Manage.*, *132*(6), 414–423, doi:10.1061/(ASCE)0733-9496(2006)132:6(414).

Cai, X., D. C. McKinney, and L. S. Lasdon (2003a), Integrated hydrologic-agronomic-economic model for river basin management, *J. Water Resour. Plann. Manage.*, *129*(1), 4–17, doi:10.1061/(ASCE)0733-9496(2003)129:1(4).

Cai, X. M., M. W. Rosegrant, and C. Ringler (2003b), Physical and economic efficiency of water use in the river basin: Implications for efficient water management, *Water Resour. Res.*, *39*(1), 1013, doi:10.1029/2001WR000748.

Cai, X., C. Ringler, and J.-Y. You (2008), Substitution between water and other agricultural inputs: Implications for water conservation in a river basin context, *Ecol. Econ.*, *66*, 38–50, doi:10.1016/j.ecolecon.2008.02.010.

Campos, J. E. G., and F. H. Freitas-Silva (1998), Hidrogeologia do distrito federal, in *Inventário Hidrogeológico e dos Recursos Hídricos Superficiais do Distrito Federal*, p. 85, Inst. Estadual de Meio Ambiente, Secr. do Meio Ambiente Ciencia y Tecnol., Univ. de Brasilia (IEMA/SEMATEC/UNB), Brasilia.

Characklis, G. W., R. C. Griffin, and P. B. Bedient (1999), Improving the ability of a water market to efficiently manage drought, *Water Resour. Res.*, *35*(3), 823–831, doi:10.1029/1998WR900094.

Characklis, G. W., B. R. Kirsch, J. Ramsey, K. E. M. Dillard, and C. T. Kelley (2006), Developing portfolios of water supply transfers, *Water Resour. Res.*, *42*, W05403, doi:10.1029/2005WR004424.

Chatterjee, B., R. E. Howitt, and R. J. Sexton (1998), The optimal joint provision of water for irrigation and hydropower, *J. Environ. Econ. Manage.*, *36*(3), 295–313, doi:10.1006/jeem.1998.1047.

Golan, A., G. G. Judge, and D. J. Miller (1996), *Maximum Entropy Econometrics: Robust Estimation With Limited Data*, John Wiley, Chichester, U. K.

Guan, D., and K. Hubacek (2007), A new and integrated hydro-economic accounting and analytical framework for water resources: A case study for North China, *J. Environ. Manage.*, *88*(4), 1300–1313, doi:10.1016/j.jenvman.2007.07.010.

Harou, J. J., and J. R. Lund (2008), Ending groundwater overdraft in hydrologic-economic systems, *Hydrogeol. J.*, *16*(6), 1039–1055, doi:10.1007/s10040-008-0300-7.

Harou, J., J. Medellin, T. Zhu, S. Tanaka, J. Lund, S. Stine, M. Jenkins, and M. Olivares (2006), Extreme drought and water supply management in California, paper presented at 2006 World Environmental and Water Resources Congress, Am. Soc. Civ. Eng., Omaha, Nebr., 21–25 May.

Harou, J. J., M. Pulido-Velazquez, D. E. Rosenberg, J. Medellin-Azuara, J. R. Lund, and R. E. Howitt (2009), Hydro-economic models: Concepts, design, applications, and future prospects, *J. Hydrol.*, *375*(3–4), 627–643.

House, R. M. (1987), USMP regional agricultural model, Natl. Econ. Div. Rep., U.S. Dep. of Agric., Washington, D. C.

Howitt, R. E. (1995), Positive mathematical programming, *Am. J. Agric. Econ.*, *77*(2), 329–342, doi:10.2307/1243543.

Howitt, R. E., and B. D. Gardner (1986), Cropping production and resource interrelationships among California crops in response to the 1985 Food Security Act, in *Impacts of Farm Policy and Technical Change on US and Californian Agriculture*, edited by H. Carter, pp. 271–290, Agric. Issues Cent., Univ. of Calif., Davis.

Howitt, R. E., and S. Msangui (2002), Reconstructing dissagregate production functions, paper presented at the American Agricultural Economics Association (AAEA) Annual Meeting, Long Beach, Calif., 28–30 July.

HydroGeoLogic, Inc. (1996), MODHMS software documentation (v. 3.0), Herndon, Va.

Jaynes, E. T. (1957), Information theory and statistical mechanics, *Phys. Rev.*, *108*, 171–190, doi:10.1103/PhysRev.108.171.

Kasnakoglu, H., and S. Bauer (1988), Concept and application of an agricultural sector model for policy analysis in Turkey, in *Agricultural Sector Modeling*, edited by S. Bauer and W. Henrichsmeyer, Wiss. Vauk, Kiel, Germany.

Krol, M., A. Jaeger, A. Bronstert, and A. Guntner (2006), Integrated modelling of climate, water, soil, agricultural and socio-economic processes: A general introduction of the methodology and some exemplary results from the semi-arid north-east of Brazil, *J. Hydrol.*, *328*(3–4), 417–431, doi:10.1016/j.jhydrol.2005.12.021.

Lance, H. L., and D. J. Miller (1998), Estimation of multioutput production functions with incomplete data: A generalized maximum entropy approach, *Eur. Rev. Agric. Econ.*, *25*, 188–209.

Lefkoff, L. J., and S. M. Gorelick (1990a), Benefits of an irrigation water rental market in a saline stream-aquifer system, *Water Resour. Res.*, *26*(7), 1371–1381.

Lefkoff, L. J., and S. M. Gorelick (1990b), Simulating physical processes and economic behavior in saline, irrigated agriculture: Model development, *Water Resour. Res.*, *26*(7), 1359–1369.

Loucks, D. P. (2006), Modeling and managing the interactions between hydrology, ecology and economics, *J. Hydrol.*, *328*(3–4), 408–416, doi:10.1016/j.jhydrol.2005.12.020.

Marques, G. F., J. R. Lund, M. R. Leu, M. Jenkings, R. E. Howitt, T. Harter, S. Hatchett, N. Ruud, and S. Burke (2006), Economically driven simulation of regional water systems: Frank-Kern, California, *J. Water Resour. Plann. Manage.*, *132*(6), 468–479, doi:10.1061/(ASCE)0733-9496(2006)132:6(468).

McDonald, M. C., and A. W. Harbaugh (1988), A modular three-dimensional finite-difference ground-water flow model, *U.S. Geol. Surv. Tech. Water Resour. Invest., Book 6, Chap. A1*, 586, pp.

Medellín-Azuara, J., J. J. Harou, M. A. Olivares, K. Madani, J. R. Lund, R. E. Howitt, S. K. Tanaka, and M. W. Jenkins (2008), Adaptability and adaptations of California's water supply system to dry climate warming, *Clim. Change*, *87*, suppl. 1, S75–S90, doi:10.1007/s10584-007-9355-z.

Mittelhammer, R. C., G. G. Judge, and D. J. Miller (2000), *Econometric Foundations*, Cambridge Univ. Press, Cambridge, U. K.

Noel, J. E., and R. E. Howitt (1982), Conjunctive multibasin management: An optimal control approach, *Water Resour. Res.*, *18*(4), 753–763, doi:10.1029/WR018i004p00753.

Panday, S., and P. S. Huyakorn (2004), A fully coupled physically based spatially distributed model for evaluating surface/subsurface flow, *Adv. Water Resour.*, *27*(4), 361–382, doi:10.1016/j.advwatres.2004.02.016.

Paris, Q., and R. E. Howitt (1998), An analysis of ill-posed production problems using maximum entropy, *Am. J. Agric. Econ.*, *80*, 124–138, doi:10.2307/3180275.

Pulido-Velazquez, M., M. W. Jenkins, and J. R. Lund (2004), Economic values for conjunctive use and water banking in southern California, *Water Resour. Res.*, *40*, W03401, doi:10.1029/2003WR002626.

Pulido-Velazquez, M., J. Andreu, and A. Sahuquillo (2006), Economic optimization of conjunctive use of surface water and groundwater at the basin scale, *J. Water Resour. Plann. Manage.*, *132*(6), 454–467, doi:10.1061/(ASCE)0733-9496(2006)132:6(454).

Ringler, C., N. V. Huy, and S. Msangui (2006), Water allocation policy modeling for the Dong Nai River Basin: An integrated perspective, *J. Am. Water Resour. Assoc.*, *42*(6), 1465–1482, doi:10.1111/j.1752-1688.2006.tb06014.x.

Rosegrant, M. W., C. Ringler, D. C. McKinney, X. Cai, A. Keller, and G. Donoso (2000), Integrated economic-hydrologic water modeling at the basin scale: The Maipo river basin, *Agric. Econ.*, *24*(1), 33–46.

Schoups, G., C. L. Addams, J. L. Minjares, and S. M. Gorelick (2006), Sustainable conjunctive water management in irrigated agriculture: Model formulation and application to the Yaqui Valley, Mexico, *Water Resour. Res.*, *42*, W10417, doi:10.1029/2006WR004922.

Tanaka, S. K., T. J. Zhu, J. R. Lund, R. E. Howitt, M. W. Jenkins, M. A. Pulido, M. Tauber, R. S. Ritzema, and I. C. Ferreira (2006), Climate warming and water management adaptation for California, *Clim. Change*, *76*(3–4), 361–387, doi:10.1007/s10584-006-9079-5.

The World Bank (2007), *World Development Report 2007: Development and the Next Generation*, Washington, D. C.

Vaux, H. J., and R. E. Howitt (1984), Managing water scarcity: An evaluation of interregional transfers, *Water Resour. Res.*, *20*(7), 785–792, doi:10.1029/WR020i007p00785.

Voinov, A., R. Costanza, L. Wainger, R. Boumans, F. Villa, T. Maxwell, and H. Voinov (1999), Patuxent landscape model: Integrated ecological economic modeling of a watershed, *Environ. Modell. Software*, *14*(5), 473–491, doi:10.1016/S1364-8152(98)00092-9.

Ward, F. A., and T. P. Lynch (1996), Integrated river basin optimization: Modeling economic and hydrologic interdependence, *Water Resour. Bull.*, *32*(6), 1127–1138.

L. H. Bassoi, Embrapa Semiárido, BR 428, Km 152, 56302-970, Petrolina, PE Brazil.

R. Howitt and S. Vosti, Department of Agricultural and Resource Economics, University of California, One Shields Ave., Davis, CA 95616, USA.

M. P. Maneta, Geosciences Department, University of Montana, 32 Campus Dr., MS 1296, Missoula, MT 59812, USA. (marco.maneta@umontana.edu)

S. Panday, AMEC Geomatrix Consultants, Inc., 620 Herndon Pkwy., Ste. 200, Herndon, VA 20170, USA.

L. Rodrigues, Embrapa Cerrados, BR 020, Km 18, 73310-970 Planaltina, DF Brazil.

M. O. Torres, Department of Economics, Catholic University of Brasília, Campus II, SGAN 916, Modulo A, Sala A-113, Brasilia, DF Brazil.

W. W. Wallender, Department of Land, Air and Water Resources, University of California, One Shields Ave., Davis, CA 95616, USA.